



## City Research Online

### City, University of London Institutional Repository

---

**Citation:** Viphavakit, C., Patchoo, W., Boonruang, S., Themistos, C., Komodromos, M., Mohammed, W. S. & Rahman, B. M. (2017). Demonstration of Polarization-Independent Surface Plasmon Resonance Polymer Waveguide for Refractive Index Sensing. *Journal of Lightwave Technology*, 35(14), pp. 3012-3019. doi: 10.1109/jlt.2017.2711959

This is the accepted version of the paper.

This version of the publication may differ from the final published version.

---

**Permanent repository link:** <https://openaccess.city.ac.uk/id/eprint/18501/>

**Link to published version:** <https://doi.org/10.1109/jlt.2017.2711959>

**Copyright:** City Research Online aims to make research outputs of City, University of London available to a wider audience. Copyright and Moral Rights remain with the author(s) and/or copyright holders. URLs from City Research Online may be freely distributed and linked to.

**Reuse:** Copies of full items can be used for personal research or study, educational, or not-for-profit purposes without prior permission or charge. Provided that the authors, title and full bibliographic details are credited, a hyperlink and/or URL is given for the original metadata page and the content is not changed in any way.

---

City Research Online:

<http://openaccess.city.ac.uk/>

[publications@city.ac.uk](mailto:publications@city.ac.uk)

---

# Demonstration of polarization-independent surface plasmon resonance polymer waveguide for refractive index sensing

CHARUSLUK VIPHAVAKIT,<sup>1,\*</sup> SAKOOLKAN BOONRUANG,<sup>2</sup> WISARN PATCHOO,<sup>3</sup> CHRISTOS THEMISTOS,<sup>4</sup> MICHAEL KOMODROMOS,<sup>4</sup> WALEED S. MOHAMMED,<sup>3</sup> AND B. M. AZIZUR RAHMAN<sup>1</sup>

<sup>1</sup>*School of Mathematics, Computer Science and Engineering, City University London, Northampton Square, London EC1V 0HB, UK*

<sup>2</sup>*Photonics Technology Laboratory, Thailand National Electronics and Computer Technology Center (NECTEC), KlongLuang, Pathumthani 10120, Thailand*

<sup>3</sup>*Center of Research in Optoelectronics, Communication and Control System (BU-CROCCS), Bangkok University, Paholyotin Rd., Klong Luang, Pathumthani 12120, Thailand*

<sup>4</sup>*Department of Electrical Engineering, Frederick University, 7 Y. Frederickou Str., Nicosia, 1036, Cyprus*

\*charusluk.v@gmail.com

**Abstract:** A gold-coated ormocomp waveguide is studied for it to be used for refractive index sensing applications. The ormocomp waveguide is fabricated using the nanoimprint method with width and height of 10  $\mu\text{m}$ . The waveguide is coated with gold of thickness 100 nm using the sputtering technique in order to introduce surface plasmon resonance at the sides and the top of the structure. Hence, a polarization-independent waveguide is achieved and the light confinement in both the TM and TE modes are studied. Supermodes occurring from the fundamental dielectric mode coupled with plasmonic supermode at the resonance peak are investigated. This paper presents the results obtained through simulations and also experimental validation. With this structure, there are two dielectric-plasmon supermodes with two resonance peaks separated by 50 nm. A red shift is observed when the refractive index of the cladding material increases. The cladding material includes water ( $n=1.333$ ) and iso-propanol solutions with refractive indices of 1.344, 1.351 and 1.365. The gold-coated ormocomp waveguide has sensitivity of about 544.55 nm/RIU with a resolution of  $5.3 \times 10^{-3}$  RIU.

© 2016 Optical Society of America

**OCIS codes:** (130.5460) Polymer Waveguides; (240.6680) Surface Plasmon; (220.4000) Microstructure Fabrication; (000.4430) Numerical approximation and Analysis; (260.5430) Polarization; (280.4788) Optical Sensing and Sensors.

---

## References

1. S. P. Chan, C. E. Png, S. T. Lim, G. T. Reed, and V. M. Passaro, "Single-mode and polarization-independent silicon-on-insulator waveguides with small cross section," *Journal of Lightwave Technology* **23**, 2103 (2005).
2. W. R. Headley, G. T. Reed, S. Howe, A. Liu, and M. Paniccia, "Polarization-independent optical racetrack resonators using rib waveguides on silicon-on-insulator," *Applied Physics Letters* **85**, 5523-5525 (2004).
3. L. Vivien, S. Laval, B. Dumont, S. Lardenois, A. Koster, and E. Cassan, "Polarization-independent single-mode rib waveguides on silicon-on-insulator for telecommunication wavelengths," *Optics Communications* **210**, 43-49 (2002).
4. H. Ma, A. Y. Jen, and L. R. Dalton, "Polymer-Based Optical Waveguides: Materials, Processing, and Devices," *Advanced Materials* **14**, 1339-1365 (2002).
5. K.-H. Haas and K. Rose, "Hybrid inorganic/organic polymers with nanoscale building blocks: precursors, processing, properties and applications," *Reviews on Advanced Materials Science* **5**, 47-52 (2003).
6. C. Sanchez, P. Belleville, M. Popall, and L. Nicole, "Applications of advanced hybrid organic-inorganic nanomaterials: from laboratory to market," *Chemical Society Reviews* **40**, 696-753 (2011).
7. C. Viphavakit, N. Atthi, S. Boonruang, C. Themistos, M. Komodromos, W. S. Mohammed, and B. M. A. Rahman, "Realization of a polymer nanowire optical transducer by using the nanoimprint technique," *Applied Optics* **53**, 7487-7497 (2014).

8. M. Fukuda, T. Aihara, K. Yamaguchi, Y. Y. Ling, K. Miyaji, and M. Tohyama, "Light detection enhanced by surface plasmon resonance in metal film," *Applied Physics Letters* **96**, 153107 (2010).
9. J. Homola, "Present and future of surface plasmon resonance biosensors," *Analytical and Bioanalytical Chemistry* **377**, 528-539 (2003).
10. J. Homola, "Surface plasmon resonance sensors for detection of chemical and biological species," *Chemical Reviews* **108**, 462-493 (2008).
11. C. Viphavakit, S. Boonruang, C. Themistos, M. Komodromos, W. S. Mohammed, and B. M. A. Rahman, "Surface plasmon resonance-enhanced light interaction in an integrated ormocomp nanowire," *Optical and Quantum Electronics* **48**, 1-15 (2016).
12. F. Liu, Y. Rao, Y. Huang, W. Zhang, and J. Peng, "Coupling between long range surface plasmon polariton mode and dielectric waveguide mode," *Applied Physics Letters* **90**, 141101 (2007).
13. M. Weisser, B. Menges, and S. Mittler-Neher, "Refractive index and thickness determination of monolayers by multi mode waveguide coupled surface plasmons," *Sensors and Actuators B: Chemical* **56**, 189-197 (1999).
14. B. M. A. Rahman and J. B. Davies, "Finite-element solution of integrated optical waveguides," *Journal of Lightwave Technology* **2**, 682-688 (1984).
15. MicroresistTechnology, "UV-Curable Hybrid Polymers for Micro Optical Components," (April, 2014).
16. P. B. Johnson and R.W. Christy, "Optical constants of the noble metals," *Physical Review B* **6**, 4370 (1972).

## 1. Introduction

Polarization-independent waveguides have been extensively studied and investigated for different applications [1-3]. There are many types of waveguides depending on the type of material used for their fabrication, such as semiconductor, glass and polymer. Silicon is the most common semiconductor used to fabricate waveguides. However, the fabrication of silicon waveguides requires cleanroom facilities and complex equipment which are costly. Glass waveguides are well-suited for simple optical detection due to their transparency, which means that there is low light absorption at the visible region. However, glass is fragile and vibration sensitive while the fabrication process of glass waveguides is difficult and very time consuming [4].

Polymer is a distinctive alternative material which can be used to build optical waveguides. Polymer waveguides have flexibility and biocompatibility [4]. Their fabrication process can be made simple and at a low cost. There are several types of polymers commonly used in photonics. Some examples are PDMS (polydimethylsiloxane), SU8, PMMA (polymethylmethacrylate) and ormocomp. The choice of what polymer to use depends on their properties and the requirements of a particular application.

Ormocomp is used in the fabrication of the waveguides in this work because it has a refractive index of 1.52 which is higher than the glass substrate ( $n=1.51$ ). It is a hybrid polymer material consisting of an inorganic backbone and organic side groups at the molecular level, unlike composite materials which are mixtures at the macroscopic level [5]. Hence, the ormocomp is a homogeneous material that combines the properties of different material classes. Ormocomp obtains its flexibility and UV-curable property from the properties of organic polymers. The hardness and the chemical and thermal stability are obtained from the properties of ceramics whereas the transparency comes from the properties of glass. Ormocomp is also known to have an easy and low processing cost using the nanoimprint technique [6, 7].

In this paper, the ormocomp waveguides are developed for refractive index sensing purposes. The sensitivity of the waveguides can be improved by coating the dielectric waveguide with a thin metal layer, which introduces surface plasmon resonance (SPR) [8-11]. Waveguides coated with a metal layer exhibit resonance coupling between the dielectric mode in the waveguides and the plasmonic mode in the metal layer [12]. The evanescent field at the dielectric/metal interface is very sensitive to the change of the cladding index, which is significant for sensing applications [13]. A 100 nm thick gold layer is coated on both the sides and on the top of the ormocomp waveguides using the sputtering technique. Therefore, the waveguide becomes polarization-independent because the oscillation of the electrons can occur horizontally at the sides (TE mode), and vertically on the top (TM mode) of dielectric/metal interfaces.

The polarization-independent gold-coated ormocomp waveguides have been studied both through numerical simulations and experimentally. A full vectorial **H**-field finite element method (FEM) is used as a numerical tool to simulate the optical modes in the waveguide structure involving the effective index, resonance wavelength and its shift in different cladding materials such as water ( $n=1.333$ ) and iso-propanol solutions ( $n=1.344, 1.351$  and  $1.365$ ). An arrangement is set up to image the optical output signal and its transmission spectrum, thus showing the experimental resonance wavelength for each cladding material. A comparison of the resonance wavelengths, where the coupling between the dielectric mode and the plasmonic supermodes occurs, from the simulations and experiment measurements are presented. The sensitivity of the fabricated waveguides and their resolutions are also calculated.

## 2. Waveguide fabrication

The ormocomp waveguides are fabricated using the nanoimprint method which is a simple and low cost technique to transfer the waveguide pattern from a hard mold onto the ormocomp layer, which is a UV-curable hybrid polymer. In this work, silicon waveguides are used as the hard mold for the nanoimprint. The silicon waveguides are usually fabricated using a photolithography technique.

There are three methods in the photolithography technique based on how the photo mask is placed, namely, contact photolithography, proximity lithography and projection photolithography. Contact photolithography is the simplest technique and it has the lowest manufacturing cost with high output solution of 1:1 magnification. Proximity photolithography has the lower resolution due to the diffraction which occurs due to the small gap between the optical mask and the photoresist layer. The projection photolithography has the highest resolution and de-magnification can be obtained allowing a sub-wavelength structure to be fabricated. However, only a small region on the photoresist layer is exposed at a time for projection photolithography, therefore a 'stepper' is required in order to move the substrate mechanically. In this work, the waveguide structure was chosen to have width and height of  $10\ \mu\text{m}$  in order to be fabricated using contact lithography to reduce the cost since sub-wavelength resolution is not required. An SEM image of the silicon waveguide fabricated using contact photolithography is shown in Fig. 1.

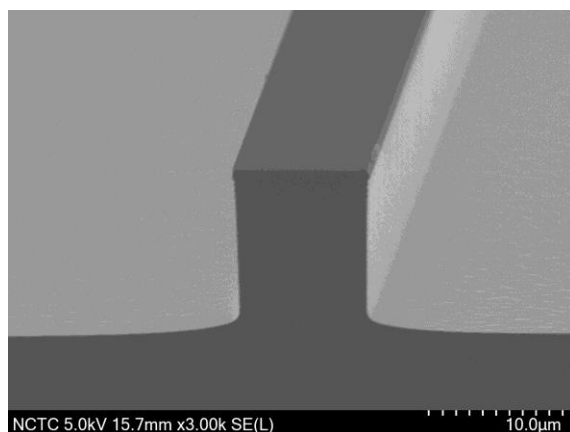


Fig. 1. SEM image of the cross section of the silicon waveguide with width and height of  $10\ \mu\text{m}$  fabricated using contact photolithography.

In order to transfer the pattern from the silicon waveguide to the ormocomp waveguide identically, polydimethylsiloxane (PDMS) is used as a soft mold, which has a reverse pattern of the waveguide as shown in Fig. 2(a). PDMS is transparent at the optical wavelengths ( $\lambda=240\ \text{nm}-1100\ \text{nm}$ ). It is prepared by mixing the silicone elastomer base (viscous liquid)

and curing agent (liquid) with a ratio of 7:1 by weight. The ratio can be varied depending on the required hardness of the PDMS mold. Liquid PDMS applied on the silicon mold has to be cured in a furnace at  $T=100^{\circ}\text{C}$  for 2 hours before it can be removed. Then, the PDMS soft mold is stamped on the ormocomp layer and cured with UV light for 5 minutes. Following the curing process, the ormocomp layer is hardened and the PDMS can be detached from the ormocomp. The nanoimprint process to fabricate ormocomp waveguide is shown in Fig. 2(b). By using the nanoimprint method, clean room facilities are not required and mass production is possible.

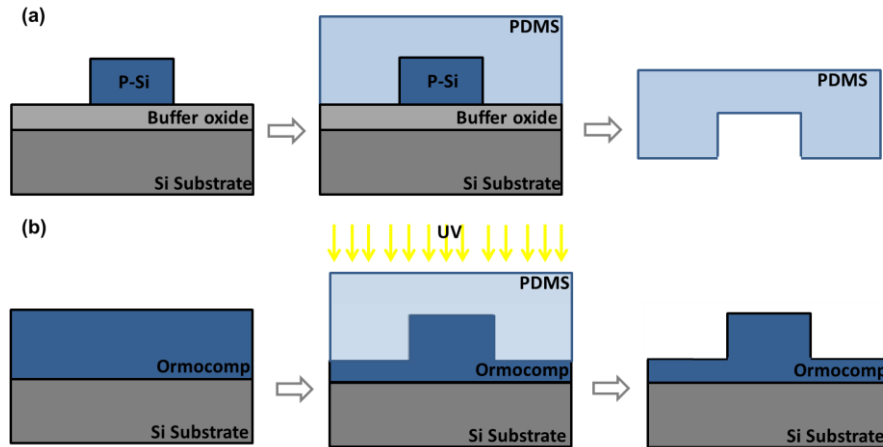


Fig. 2. (a) Schematic of PDMS soft mold preparation process for the nanoimprint technique. (b) Schematic showing the process of the nanoimprint technique for the ormocomp waveguide fabrication.

The fabricated ormocomp waveguide is proposed to be used for refractive index sensing applications. The sensing area is at the core/cladding interface where the evanescent field interacts with the analyte material. When the core of the waveguide is large enough, then light is mostly confined in the core and thus only a small amount of the evanescent field is extended into the cladding region. In order to enhance the field at the core/cladding interface, a thin gold layer is coated onto the ormocomp waveguide to introduce surface plasmon resonance (SPR). Gold is coated using the sputtering technique. In this paper, chromium layer with thickness of 5 nm is coated first as an adhesion layer. The thickness of the gold is about 100 nm. An SEM image and a magnification of the gold-coated ormocomp waveguide are shown in Fig. 3.

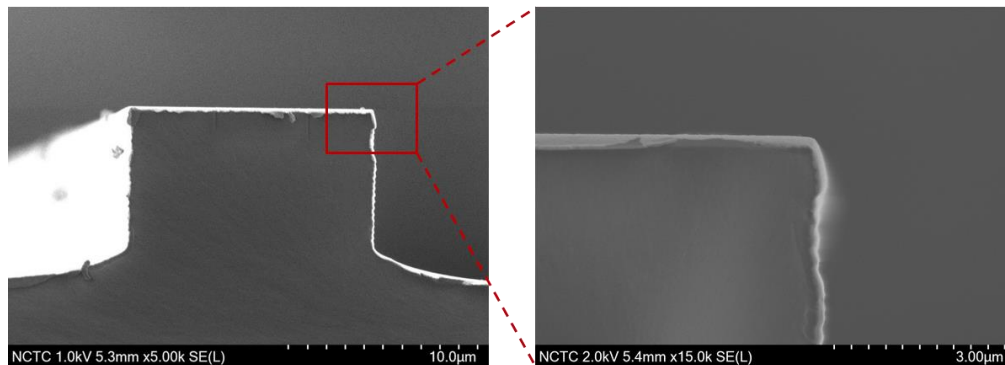


Fig. 3. SEM image of the cross section of the 10 μm wide ormocomp waveguide coated with 100 nm thick gold layer. The magnified image shows that the gold layer is coated both at the sidewall and the top surface.

It can be seen from Fig. 3 that gold is coated both on the top surface and at the sides of the waveguide allowing electrons to be excited and oscillated both vertically (top surface) and horizontally (sides surface) at the interface between the dielectric and conductive materials. Hence, the waveguides can be polarization-independent. However, both quasi-TM (vertical polarization) and quasi-TE (horizontal polarization) modes are investigated in the numerical simulations by using the Finite Element Method (FEM) in order to study the characteristics and differences between the two polarization modes.

### 3. Simulation results

The Finite Element Method (FEM) is one of the most powerful numerical techniques used to analyze complex structure problems such as optical waveguides because of its accuracy, flexibility and versatility in the numerical analysis of optical waveguides. In the present work the full-vectorial  $\mathbf{H}$ -field finite element formulation has been applied for the modal analysis of the quasi-TM and quasi-TE modes in the gold coated waveguide to determine the propagation characteristics of the coupled dielectric-plasmonic mode.

The principle of the FEM is to divide the complex structure into discrete elements, thus an equivalent discrete model for each element is constructed and all the elemental contributions to the system may be assembled to get an approximate solution of those differential or integral equation problems. Various types of elements can be used to assemble the continuum complex element, such as for example, triangles, rectangles, etc. However, the triangle shaped element is the most preferable because it has the simplest shape that can fit any complicated structures. The functional used to solve the problem is related to standard eigenvalue problems, and the modal characterization is obtained by minimizing the functional given in Eq. (1) [14]:

$$\omega^2 = \frac{\int [(\nabla \times \mathbf{H})^* \cdot \epsilon^{-1} (\nabla \times \mathbf{H}) + p (\nabla \times \mathbf{H})^* (\nabla \times \mathbf{H})] dx dy}{\int \mathbf{H}^* \cdot \mu \mathbf{H} dx dy} \quad (1)$$

where  $\mathbf{H}$  is the full vectorial magnetic field, \* represents a complex conjugate and transpose,  $\omega$  is the angular frequency of the wave,  $\omega^2$  is the eigenvalue, and  $\epsilon$  and  $\mu$  are the permittivity and permeability, respectively.

In this work, 64800 first order triangular elements are used to represent one half of the gold-coated waveguide structure. The waveguide has a width and height of 10  $\mu\text{m}$  with 100 nm thick gold layer coated at the sides and on the top. With FEM, the size of the triangles can be varied for each individual part of the waveguide to achieve high computational efficiency. In this case, vertical resolution of 1.67 nm is obtained for the 100 nm thick gold layer. The ormocomp waveguide with refractive index of 1.52 has a high transparency, which means there is low light absorption at the visible wavelength [15]. Hence, the operating wavelength in this work is 400-700 nm. The complex refractive index of gold in the visible region is based on Johnson and Christy study [16]. For the sensing applications purposes, FEM is used to study the waveguide with different refractive indices of the cladding region. The refractive indices of the cladding region examined, have values of 1.333, 1.344, 1.351 and 1.365 which represent water and different concentrations of isopropanol solutions, respectively.

From the SEM image of the fabricated gold-coated ormocomp waveguide, gold is coated both at the sides and on the top of the ormocomp. Therefore, the light propagating in the waveguide is studied for both the quasi-TM mode and quasi-TE modes using the full vectorial  $\mathbf{H}$ -field FEM. Changes in the effective index of a fundamental guided mode over the visible region for the quasi-TM and quasi-TE modes are shown in Fig. 4.

The effective index of the gold-coated ormocomp waveguide is decreased with larger operating wavelength because the small wavelength can confine more inside the waveguide compared to the large wavelength. However, the ormocomp waveguide structure is larger than the operating wavelength in this case, so there is no cut-off in this waveguide configuration.

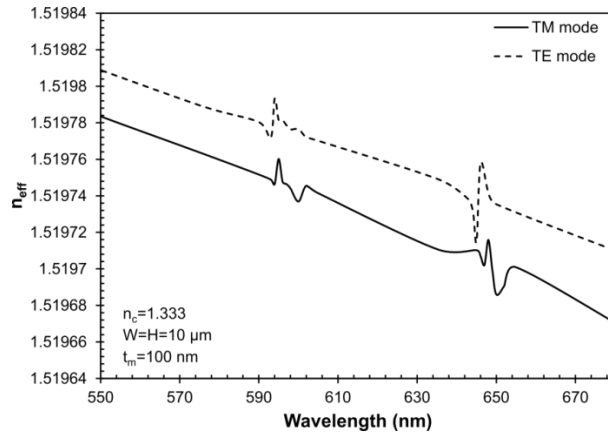


Fig. 4. Change of effective indices over the operating wavelength in the visible region for quasi-TM and quasi-TE modes.

The effective index variation graph shows particular peaks in some specific locations indicating the resonance phenomena. The effective index of the plasmonic mode is usually higher than the one of the dielectric mode. Therefore, the coupled mode between plasmonic and dielectric modes occurring at the resonance wavelength is higher than the dielectric mode alone at the non-resonance wavelengths. The thickness of the gold layer is 100 nm, which is thick enough to allow fundamental and higher order plasmonic modes to be supported. The different orders of the plasmonic modes can be coupled with the dielectric mode at different resonance wavelengths leading to several resonance peaks to occur. The thickness of the gold layer is fixed at 100 nm because with thinner gold layers, the plasmonic modes cannot occur. In addition, the effective index of the quasi-TE mode is slightly higher than the quasi-TM mode because there are two metal/cladding interfaces at the sides of the ormocomp waveguide for the quasi-TE mode but only one metal/cladding interface for the quasi-TM mode which is on the top of the waveguide. However, the resonance wavelengths occurring at both the quasi-TM and quasi-TE modes are almost identical.

The 2D optical fields obtained from the  $\mathbf{H}$ -field FEM compared with the optical field images from the experiment and the field presented on the  $y$ -axis at the non-resonance wavelength and the resonance wavelength are shown in Fig. 5 and Fig. 6, respectively.

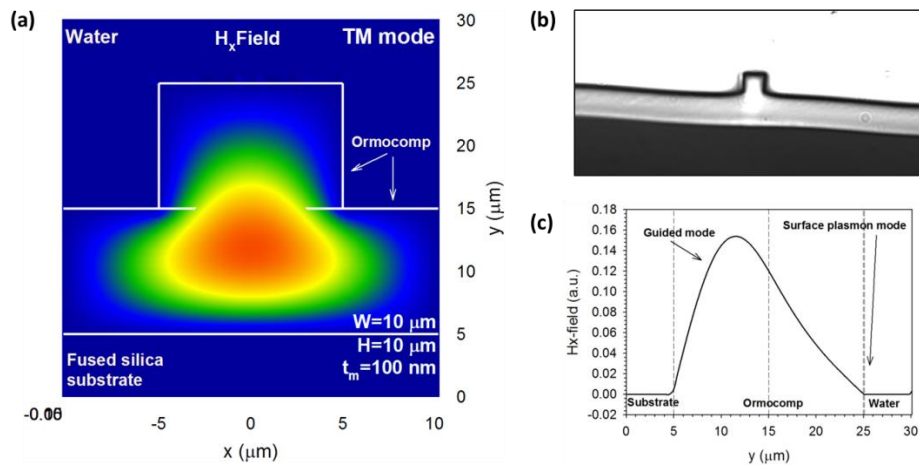


Fig. 5. Modal field profile excited in the ormocomp waveguide at non-resonance wavelengths from (a) FEM simulation and (b) experiment, and (c)  $H_x$  field of the guided mode along the  $y$ -axis.

From Fig. 5, only the dielectric mode is significant and confined in the core of the gold-coated ormocomp waveguide at the non-resonance wavelength. The ormocomp waveguide has a rib-structure, so some of the light at the core of the waveguide is extended into the rib layer as can be seen from the simulation in Fig. 5(a) and the image from CCD camera in the experimental setup in Fig. 5(b).

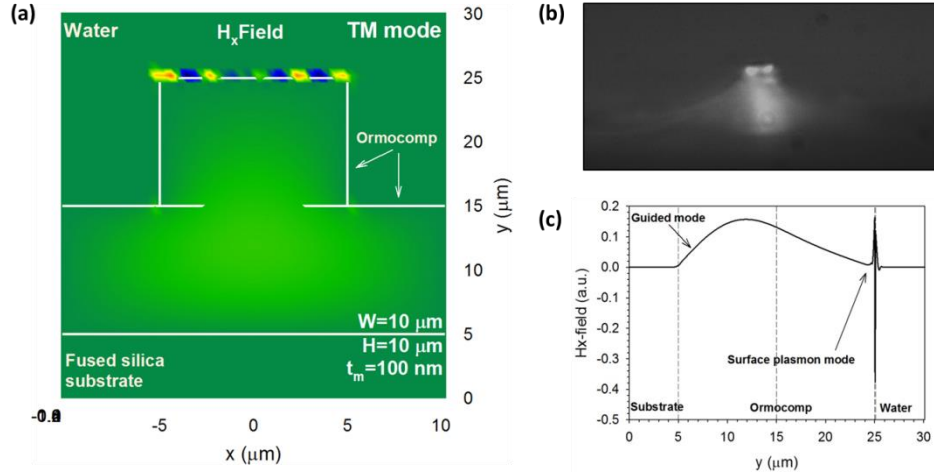


Fig. 6. Modal field profile excited in the ormocomp waveguide at the resonance wavelength from (a) FEM simulation and (b) experiment, and (c)  $H_x$  field of the coupled dielectric-plasmonic mode along the  $y$ -axis.

At the resonance wavelength, the plasmonic modes are introduced and coupled with the dielectric mode to become a supermode. The optical image from the CCD camera in the experiment, Fig. 6(b), shows a good agreement to the simulation result, shown in Fig. 6(a), in which both the plasmonic mode at the metal/cladding interface and the dielectric mode confined in the core and rib layer are presented. The plasmonic mode is stronger than the dielectric mode which is clearly seen from the optical field along the  $y$ -axis in Fig. 6(c). On the other hand, the dielectric mode is dominant at the non-resonance wavelength but the plasmonic mode is dominant at the resonance wavelength. In addition, the gold-coated ormocomp waveguide has two dielectric/electric interfaces which are the ormocomp/gold and the cladding/gold interfaces. Therefore, the plasmonic modes occurring at the metal layer are also plasmonic supermodes. According to the large surface plasmon mode at the resonance wavelength, the power confinement in the sensing region is also expected to be improved. By using the FEM simulation, the graph showing the normalized power confinement in the sensing region, which is the metal/cladding interface, is presented in Fig. 7.

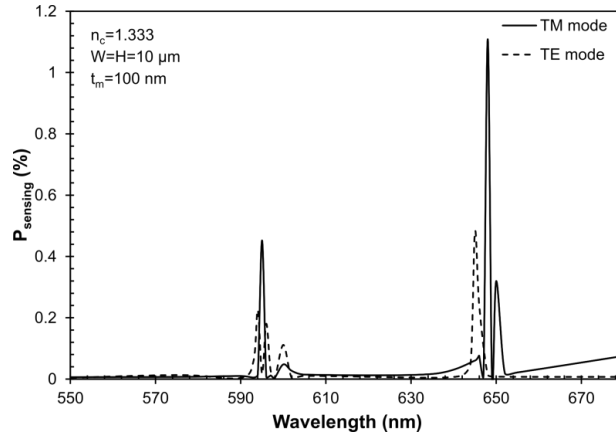


Fig. 7. Graph of normalized power confinement in the sensing region of the ormocomp waveguide in water cladding calculated by using an in-house FEM program for quasi-TM and quasi-TE modes.

The resonance wavelength can be indicated from power confinement in the sensing region graph where the peaks representing high power confinement are occurred. There are several peaks occurring due to the thickness of the gold layer. Considering the highest peak, there are two distinguished peaks for both the quasi-TM and the quasi-TE modes in the 100 nm gold layer. The resonance peak wavelengths of the quasi-TM and quasi-TE modes, of the gold-coated ormocomp waveguide, in different cladding materials, are presented in Table 1.

**Table 1: Simulation results of the resonance peaks of the gold-coated ormocomp waveguide in different cladding materials for quasi-TM and quasi-TE modes.**

n	TM mode		TE mode	
	Resonance peak 1	Resonance peak 2	Resonance peak 1	Resonance peak 2
1.333	595 nm	648 nm	594 nm	645 nm
1.344	599 nm	653 nm	599 nm	652 nm
1.351	603 nm	655 nm	603 nm	653 nm
1.365	610 nm	661 nm	611 nm	662 nm

The resonance peaks for both the quasi-TM and quasi-TE modes occur at almost the same wavelength because of the designed waveguide structure leads to a small difference in their effective indices. Two resonance peaks are located about 50 nm away from each other. The resonance peaks for each cladding material in Table 1 can be plotted as shown in Fig. 8.

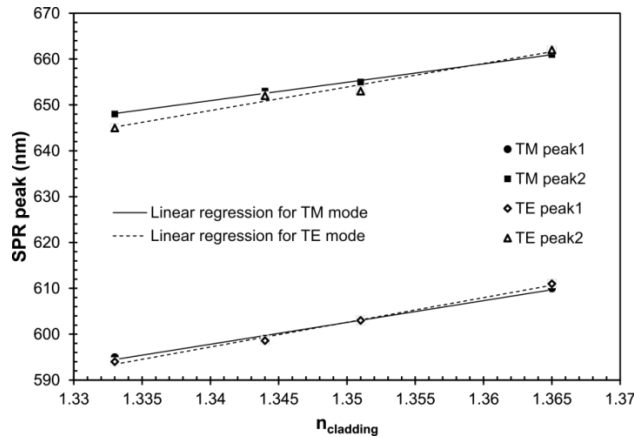


Fig. 8. Graph of the two resonance peaks obtained from the numerical simulations for each cladding material in both the quasi-TM and quasi-TE modes.

It can be observed from Fig. 8 that the resonance peak wavelength has a linear relationship with the refractive index of the cladding material for both the quasi-TM and quasi-TE modes. The regression lines of the quasi-TM modes, which are represented by solid lines, nearly perfectly fit the data with R-squared of 0.9929 and 0.9960 for resonance peaks 1 and 2, respectively. For the quasi-TE modes, the regression lines are represented by dashed lines with R-squared of 0.9755 and 0.9935 for resonance peaks 1 and 2, respectively. The slopes of the quasi-TE modes are slightly higher than the slopes of the quasi-TM mode for both resonance peaks which means that the quasi-TE mode has higher sensitivity compared to the quasi-TM mode. This is due to the larger surface area (double) at the sides of the waveguide compared to the surface area on the top.

#### 4. Experimental results

The experiment part includes an optical setup for imaging the optical output signal and monitoring the transmission spectrum from the gold-coated ormo-comp waveguide to observe the resonance peak and its shift when there is a change in refractive index of the cladding material. The ormo-comp waveguides with width and height of 10  $\mu\text{m}$  are fabricated using the nanoimprint technique and coated with 100 nm gold layer using the sputtering method. The cladding materials in the experiment are water and iso-propanol solutions with different concentrations. The iso-propanol solutions are a mixture of water and iso-propanol with the volume ratio of 1:1, 1:3 and 1:5, providing the refractive indices of 1.365, 1.351 and 1.344, respectively.

The optical setup to image the output signals and monitor the transmittance spectrum from the waveguide structures mainly consists of a broadband light source, objective lens with 10x and 20x magnifications, a polarizer, a cube beam splitter, two CCD cameras and a compact CCD spectrometer as shown in Fig. 9.

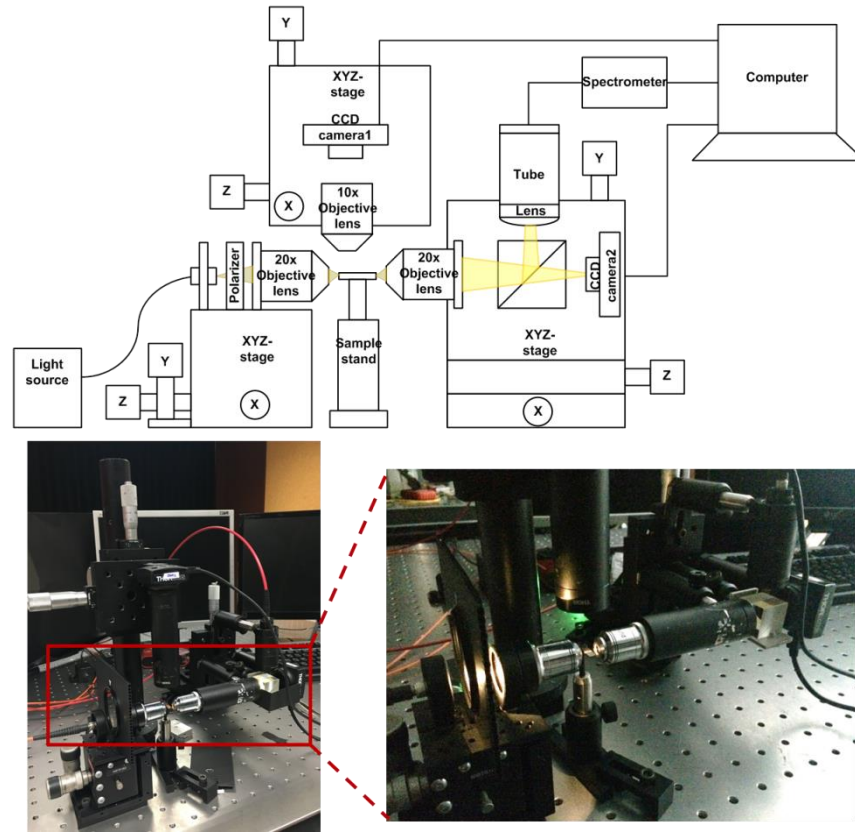


Fig. 9. Optical setup for imaging and measuring the transmitted output signal.

The broadband light source used in the optical set up is the warm white LED type connected to multimode fiber (Thorlabs: MWWHF1). The light then passes through a polarizer in order to study the TM and TE modes separately by rotating the polarizer by  $90^\circ$ . After that, the light is focused into the gold-coated ormocomp waveguide using the 20x objective lens. An alignment setup is placed above the sample stand by having 10x objective lens connected with the CCD camera. Through alignment, the light can propagate along the selective gold-coated ormocomp waveguide. The optical output signal is divided in half by a 50:50 split ratio cube beam splitter which can be operated in the visible region ( $\lambda=400-700$  nm). One half of the output signal is imaged by CCD camera as can be seen in Fig. 5b) and Fig. 6b) and the other half is detected by the compact spectrometer to monitor its transmittance. The transmitted output signal is used to study the resonance peak which can occur when the momentum of electron oscillation matches the momentum of the photons in the incident light. At some specific wavelength, supermodes occur due to the fact that the dielectric mode is coupled with the plasmonic mode. In addition, the plasmonic mode itself is also a supermode from the coupling between the plasmonic mode at the ormocomp/gold interface and the cladding/gold interface. There are two distinguished dielectric-plasmonic supermodes that can be observed in the experiment. The gold-coated ormocomp waveguides are tested with 4 different cladding materials, which are water and three different volume ratios of iso-propanol solutions with refractive index of 1.333, 1.344, 1.351 and 1.365, to study the resonance peaks and their shifts. The resonance peaks for both quasi-TM and quasi-TE modes of the gold-coated ormocomp waveguides in different cladding materials obtained from the experiment are presented in Table 2.

**Table 2: Experimental results of the resonance peaks of the gold-coated ormocomp waveguide in different cladding materials for the TM and TE modes.**

n	TM mode		TE mode	
	Resonance peak 1	Resonance peak 2	Resonance peak 1	Resonance peak 2
1.333	592.3397 nm	649.2628 nm	598.0099 nm	646.8102 nm
1.344	601.8363 nm	654.3479 nm	600.6294 nm	649.9333 nm
1.351	606.3138 nm	656.3691 nm	601.6343 nm	654.1263 nm
1.365	609.9699 nm	660.5675 nm	612.5647 nm	659.6628 nm

It can be seen that the resonance peaks occur in both the quasi-TM and quasi-TE modes at a similar wavelength. Hence, a polarization-independent gold-coated ormocomp waveguide has been successfully fabricated. The resonance peaks from Table 2 can be plotted so that we have a comparison with the resonance peaks obtained from the simulation using full vectorial **H**-field FEM as shown in Fig. 10.

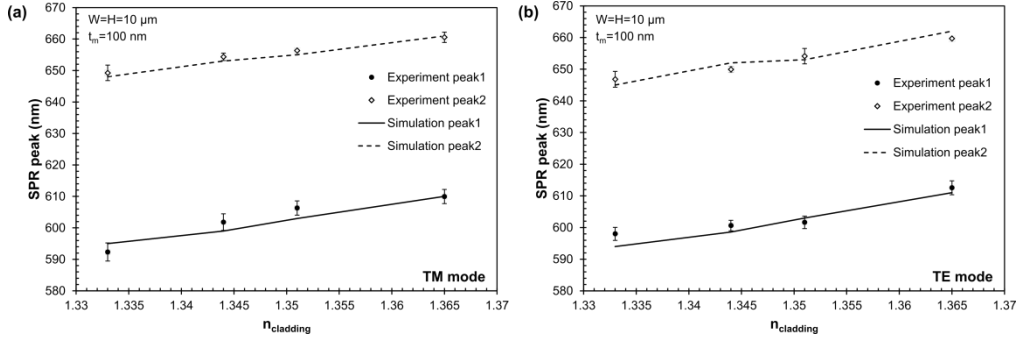


Fig. 10. Comparison of the resonance peaks obtained from the experiment and simulation for both TM and TE modes.

It can be seen from Fig. 10 that the resonance peaks obtained from the experiment have a similar trend compared to the simulation results. There are two different resonance peaks in both the experimental and simulation results, which means that there are two different plasmonic supermodes that are coupled with the dielectric mode. The two resonance peaks are located about 50 nm away from each other. The quasi-TM and quasi-TE mode have similar resonance wavelengths so the polarization in the experiment can be removed because the waveguides are polarization independent. Both experimental and simulation results show a redshift when the refractive index of the cladding material is increased.

To use this gold-coated ormocomp waveguide for refractive index sensing applications, the sensitivity is calculated from the linear regression of the experimental results and it is found to be 544.55 nm/RIU with resolution  $5.3 \times 10^{-3}$  RIU. The sensitivity and resolution of the waveguide can be further improved by optimizing the dimensions of the waveguide itself and the thickness of the gold layer. In addition, surface roughness is also considered to be one of the important parameters to improve sensitivity and resolution.

## 5. Summary

A polarization-independent gold-coated ormocomp waveguide is studied for refractive index sensing purposes. The ormocomp waveguides are fabricated using the nanoimprint method, which is considered to be simple and has low manufacturing costs without the need of cleanroom facilities. The hard mold of the ormocomp waveguides are silicon waveguides. With the dimension of  $10 \mu\text{m}$  width and height, the silicon waveguides can be fabricated using contact photolithography. With these techniques, mass production of ormocomp waveguides is possible. Gold is coated on the ormocomp waveguides at the sides and the top

surface introducing surface plasmon resonance in both horizontal (TE mode) and vertical polarizations (TM mode). The gold-coated ormocomp waveguides are studied with four different cladding materials which are water ( $n=1.333$ ) and iso-propanol solution with different concentration having refractive indices of 1.344, 1.531 and 1.365. The resonance peaks were investigated both by simulation and experimentally. An in-house full vectorial  $\mathbf{H}$ -field FEM tool is used in the simulation work. The resonance peaks occur at the wavelength where the dielectric mode couples with the plasmonic supermode. There are two resonance peaks observed because there are two different plasmonic modes coupled with the dielectric modes. Both the TM and TE modes have almost identical resonance wavelength for each cladding material. Hence, the polarization is not required and polarization-independent waveguides are achieved. The simulation and experimental results show a good agreement to each other in term of imaging, resonance peaks and their shift. With larger refractive index of the cladding material, redshift occurs. The sensitivity of the gold-coated ormocomp waveguide is around 544.55 nm/RIU, and the resolution is  $5.3 \times 10^{-3}$  RIU and these can be further improved.